Diyala Journal of Engineering Sciences

Journal homepage: https://djes.info/index.php/djes

ISSN: 1999-8716 (Print); 2616-6909 (Online)

Comparative Fatigue Crack Growth Analysis of Modified Single-Edge-Notched Bend Specimens under Three- and Four-Point Loading using Finite Element Modeling

Abdulnaser M. Alshoaibi*, Yahya Ali Fageehi

Department of Mechanical Engineering, College of Engineering and Computer Sciences, Jazan University, Jazan 45142, Saudi Arabia.

ARTICLE INFO

Article history:
Received 08/11/2025.
Revised 03/01/2026.
Accepted 21/01/2026.
Available online: 15/03/2026.

Keywords:
Finite element method
Fatigue crack growth
Three-Point and Four-Point Bending specimens
Geometric Discontinuity
Maximum Bending Moment

ABSTRACT

In engineering components with geometric discontinuities, the fatigue crack growth of structures subjected to cyclic loading is of utmost importance. This study numerically investigates the modified Single Edge Notched Bend (SENB) specimen with a hole adjacent to the crack tip under three-point bending (3SENB) and four-point bending (4SENB) conditions. The Finite Element Method (FEM) was implemented using ANSYS Workbench 19.2. Specialized meshing was performed to determine the stress field and predict the fatigue crack propagation using the Paris' Law. This study quantitatively compares the effects of these two loading conditions on the fracture mechanics parameters of this non-standard geometry for the first time. The findings indicate that the specimen response is significantly different; the 3SENB configuration, with twice the maximum bending moment of the 4SENB, has 1.931 times the maximum von Mises stress, 1.823 times the maximum von Mises strain, and 1.965 times the stress intensity factor. The main contribution of this analysis is the development of a strong and quantifiable correlation between the maximum bending moment, and the fracture severity as defined by this work. Consequently, the predicted fatigue life of the 3SENB specimen is substantially reduced due to higher stress intensity factors. It has been found that the selection of bending configuration has a decisive and quantifiable influence on fatigue life of the modified SENB specimen with a geometric discontinuity under the specified loading condition.

1. INTRODUCTION

The ability of any engineering structure to maintain its integrity and last for a reasonable time is defined by its fatigue and fracture resistance. The primary cause of failure in crucial components in aerospace, civil, and engineering sectors [1, 2]. Fracture mechanics is the theory we use to offer predictions for structural durability by crack initiation and propagation [3, 4]. A key part of this analysis is carrying out experimental characterization of material properties, which is mostly done by standardized testing methods, like the SENB specimen in three-point bending (3PB) or four-point bending (4PB) configuration [5]. Choosing between the 3PB and 4PB setups is important as it determines the stress state and moment distribution in the sample [6]. The maximum bending moment occurs at a single point directly below the centre load in the three-point ending test. This involves a strong stress field with a high likelihood of experiencing Mode I (opening) fracture [7, 8]. On the other hand, the four-point bending test creates a location with a constant bending moment between its two inner loading points, which is often preferred because it gives a state of stress that is more uniform over a larger volume [9]. New studies show that 3PB is simpler but 4PB is more representative of real-world loading conditions. Also, in some Materials mainly functionally graded materials (FGM), 4PB can lead to mixed-mode loading (KI and KII) which might complicate the analysis but provide a better insight of failure mechanism [10]. The stress fields from these two configurations would lead to different SIFs and thus different predicted fatigue crack growth rates and total life [11]

Due to the complexity of tests and high cost of doing fatigue monitoring tests via experiments, numerical simulation from the FEM has become an invaluable and highly precise tool for fracture mechanics [12].

* Corresponding author's Email: alshoaibi@jazanu.edu.sa, alshoaibi@gmail.com.
DOI: 10.24237/djes.2026.19103

Commercial software packages, especially ANSYS Workbench, boasts elaborate procedures for modeling complex crack growth that also incorporates an advanced fatigue life prediction model, Paris' Law [13, 14]. The precision of these simulations depends on painstaking modeling techniques, specifically owing to the use of meshing strategies. These days, the crack growth feature of SMART (Separating, Morphing, Adaptive and Remeshing Technology) in ANSYS or local mesh refinement with sphere of influence are commonly employed in modern FEA (Finite Element Analysis) methods for the reliable estimation of SIFs [15, 16]. Different numerical schemes have been successfully employed to study the effect of varying parameters such as load ratio, materials properties and specimen geometry on fatigue crack growth in standard SENB and other notched specimens [17, 18]. While there have been numerous studies on standard SENB specimens, there is a significant research gap surrounding the modified SENB specimens having geometric discontinuities, such as holes close to the crack path. Such features are not merely academic; they are ubiquitous in engineering practice (e.g., fastener holes, inspection ports) and fundamentally alter the local stress field, leading to non-standard crack propagation behavior that cannot be reliably predicted by standard fracture models [19, 20].

Previous studies have investigated the use of non-standard specimen configurations in fracture mechanics. For instance, Ferreira et al. [21, 22] proposed test protocols and new formulations for fracture toughness characterization using non-standard four-point bending specimens, comparing them with standardized three-point bend geometries. Similarly, Pereira et al. [23] utilized non-standard three-point bending specimens in their numerical and experimental validation of mixed-mode fracture. However, to the best of the authors' knowledge, a detailed quantitative comparison specifically focusing on the effects of 3SENB versus 4SENB loading on the stress intensity factors, maximum von Mises stress, and predicted fatigue life for an SENB specimen modified with a hole near the crack tip has not been previously reported.

Therefore, the objective of this study is to perform a comparative numerical analysis of a modified SENB specimen, featuring a hole near the crack tip, under both three-point and four-point bending configurations using ANSYS Workbench. The research gap addressed by this work is the absence of a systematic, direct comparison of the effect of the load application point (3PB vs. 4PB) on the key fracture mechanics parameters, specifically the crack path, von-Mises stress and strain distributions, Stress Intensity Factors, and fatigue life in a modified SENB specimen with a geometric discontinuity. The novelty of this work is the direct, side-by-side comparison of the numerical results from 3PB and 4PB tests on a non-standard, modified SENB geometry, which provides a unique, quantitative demonstration of the influence of the loading configuration on the stress field and fracture parameters. This perspective sheds light on structural integrity evaluation by establishing a firm connection between the maximum bending moment and fracture in complex geometry.

2. NUMERICL ANALYSIS USING ANSYS WORKBENCH

The latest feature of ANSYS Mechanical, called SMART, that tackles complex crack propagation problems is Separating, Morphing, Adaptive, and Remeshing Technology. The modelling of crack initiation, growth, and fracture is a difficult challenge. In a SMART approach, mesh updating is automated. This is a remeshing based method which does not remesh the entire domain but remesh only the crack-front region as the crack progresses. This design makes the method more efficient than global remeshing based methods. SMART can mimic 3D crack growth and enable mixed-mode crack growth analysis for Mode I and Mode II it is ideal for the SENB specimens studied here where crack path deflection was expected due to the eccentric hole.

The Unstructured Mesh Method (UMM) complements the SMART feature. In the past, structured hex meshes were essential for accurate (SIF) calculation, but it is difficult to generate them for complex geometries, and they are very time-consuming. UMM addresses this issue by providing automatic high-fidelity all-tet meshes for crack fronts. This innovation greatly reduces pre-processing times, which previously took days, to as little as minutes. Further, the accuracy of tetrahedral meshes in estimating fracture mechanics parameters is very similar to structured meshes. The user employed high-order tetrahedron elements and used UMM-based meshing in this study using the most modern and commercial FEA software available for carrying out 3D fatigue problems. The parameters and limitations of the methodology need to be properly defined.

The SMART crack growth feature, when calculating the fatigue life according to Paris' Law, relies on stringent assumptions (namely that the material behaviour is linear elastic isotropic, and only LEFM is used in the analysis). It is assumed that plasticity at the crack tip, non-linear geometry effects, and crack-tip closure are not considered in the analysis. This shape restriction agrees with the material hypothesis of the SAE 1020 steel metal that is used for the experiment. The SMART crack growth feature, when calculating the fatigue life according to Paris' Law, relies on

stringent assumptions (namely that the material behaviour is linear elastic isotropic, and only LEFM is used in the analysis). It is assumed that plasticity at the crack tip, non-linear geometry effects, and crack-tip closure are not considered in the analysis. This shape restriction agrees with the material hypothesis of the SAE 1020 steel metal that is used for the experiment.
The modified 4SENB configuration investigated here is based on the experimental results reported by Miranda et al. [24]. As shown in Figure 1, the geometry consists of an SENB specimen with a 5.2 mm radius hole located at an eccentric distance of 9.3 mm from the notch line, subjected to four-point bending loads.
A second configuration, designated as the three-point bend specimen (3SENB), was also analyzed. While the specimen dimensions remain constant, the loading is modified to a single concentrated force applied at the center of the upper span. The 4SENB and 3SENB specimens were loaded with 10 kN and 20 kN, respectively. These specific load values were selected to maintain parity in the total load experienced by each specimen, allowing for a direct comparison of the different bending configurations.

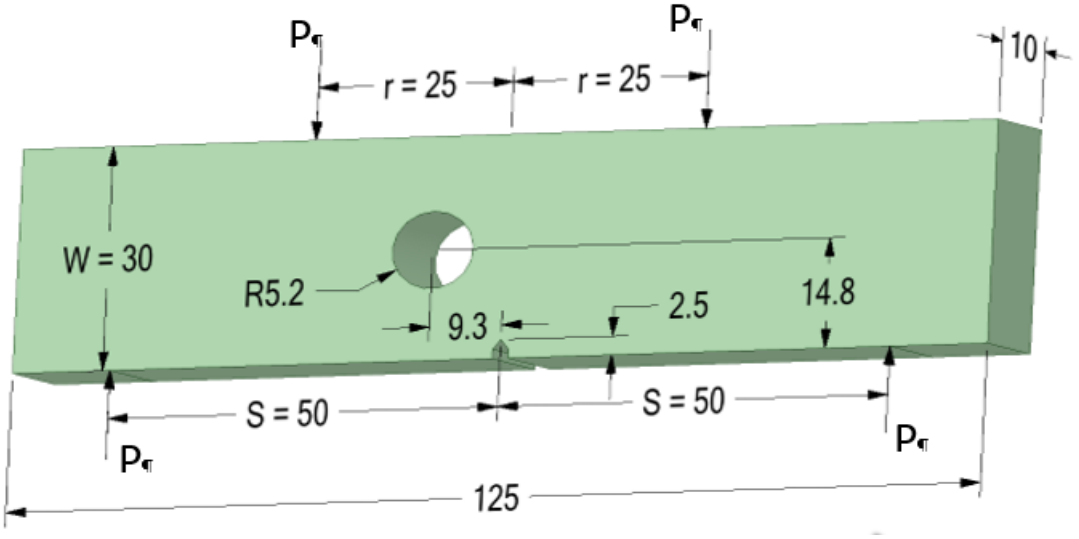

Figure 1. Geometry of the modified SENB (dimensions in mm)

As per Miranda et al.'s [24] experimental work, the behaviour of the material is assumed to be isotropic and linear elastic. Table 1 contains the important material properties which are used in the simulation. The finite element mesh was generated using ANSYS Workbench using the Unstructured Mesh Method (UMM). The mesh type used high-order tetrahedral elements. To achieve highly accurate calculation of stress intensity factors (SIFs), which depend on resolving the asymptotic stress field at the crack tip, refinement strategy will be adopted. The 4SENB specimen crack path predicted with the Quebra 2D finite element software was validated with experimental and numerical results in the literature, Miranda et al. [24]. To ensure the fidelity of the numerical results, a comprehensive mesh sensitivity study was conducted to identify an optimal element size that balances computational efficiency with predictive accuracy. This process is fundamental to the Finite Element Method (FEM), ensuring that the solution is independent of the mesh discretization. The mesh was systematically refined, starting from an element size of 1.5 mm, which yielded a Stress Intensity Factor (K_I) of 2289 MPa $mm^{0.5}$. Further refinement to 1.2 mm and 1.0 mm produced K_I values of 2826 and 2939 MPa $mm^{0.5}$, respectively. The convergence of the solution was confirmed by a marginal 4% deviation between the final two refinements, validating the stability of the numerical model as shown in Figure 2. The final mesh density configurations used for the comparative analysis are provided in Table 2 and displayed in Figures 3 and 4 respectively.

Table 1. Mechanical properties for SAE 1020 Steel [24]

Property	Value
Modulus of Elasticity	205 GPa
Poisson's Ratio	0.29
Yield Strength	285 MPa
Ultimate Strength	491 MPa
Paris' Law Coefficient, *C*	8.59×10^{-14}
Paris' Law Exponent, *m*	4.26

Table 2. Mesh density configuration for comparative analysis

Modified SENB Specimen	Number of Nodes	Number of Elements
4SENB specimen	163026	113352
3SENB specimen	154655	107472

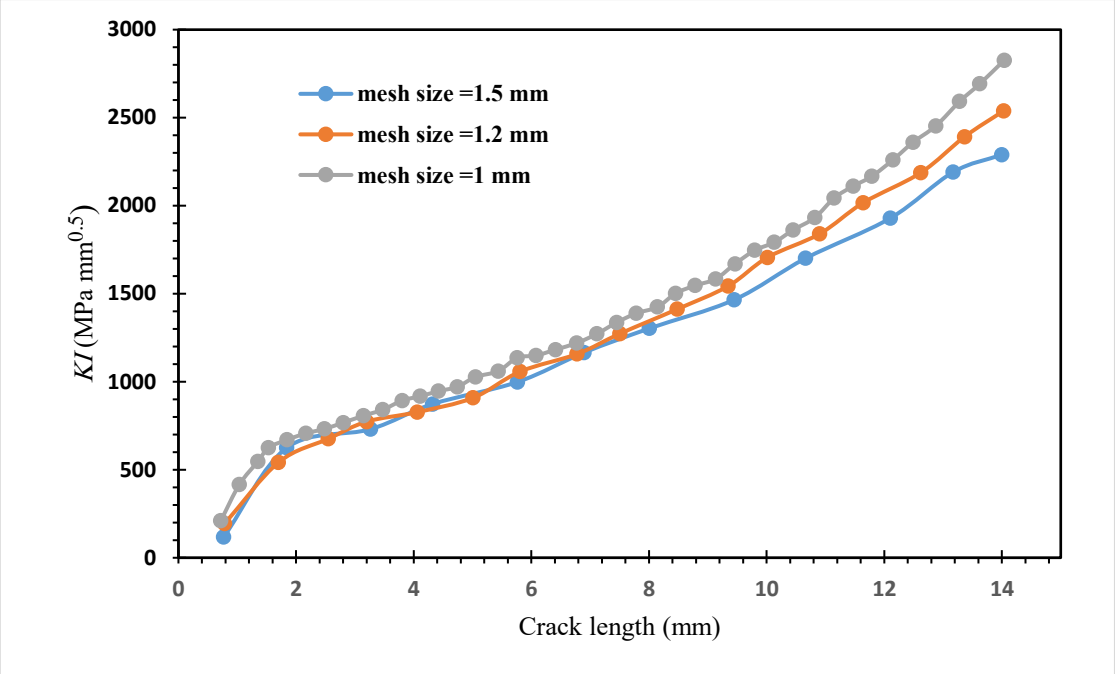

Figure 2. Mesh convergence analysis.

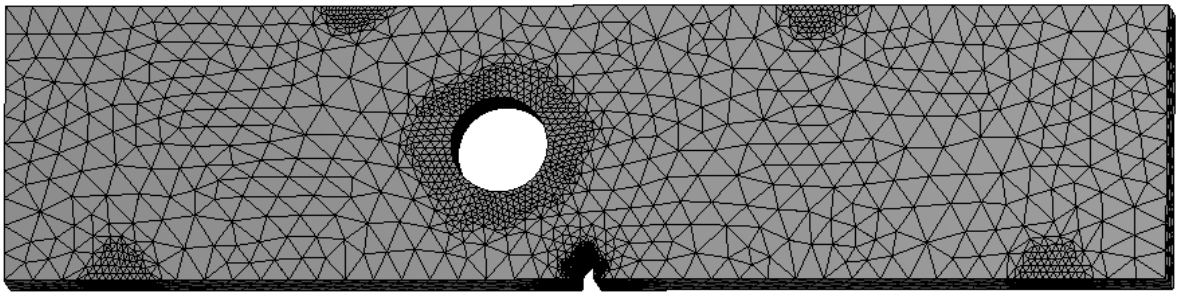

Figure 3. Meshed geometry of the 4SENB specimen.

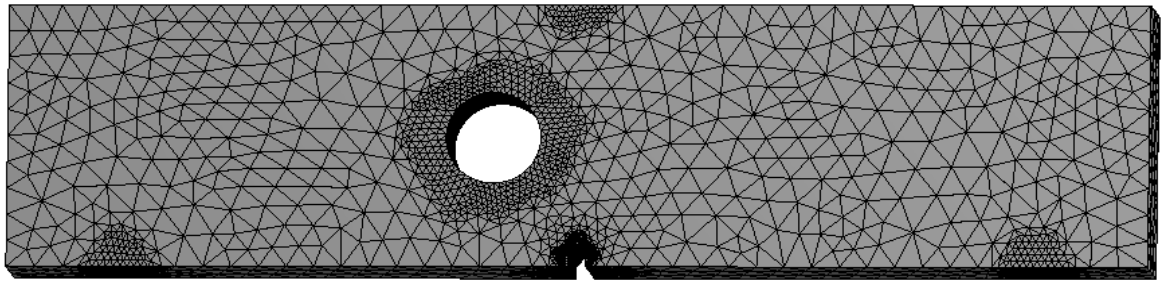

Figure 4. Meshed geometry of the 3SENB specimen

3. RESULTS AND DISCUSSION

The predicted crack path for the 4SENB specimen was validated with existing experimental and numerical results using Quebra 2D finite element software achieved by Miranda et al. [25]. The present ANSYS simulation showed excellent agreement with the reference work, with the crack propagating in the same direction as shown in Figure 5. A comparative analysis of the crack paths for the 3SENB and 4SENB specimens (Figure 6) revealed that the paths were nearly identical. This suggests that, within the studied range of load application points (r = 0 mm for 3SENB and r = 25 mm for 4SENB), the specific position of the load application point r does not exert a considerable influence on the crack path direction. Conversely, the total deformation was significantly affected, with the 3SENB specimen experiencing a 46% increase compared to the 4SENB specimen (Figure 7).

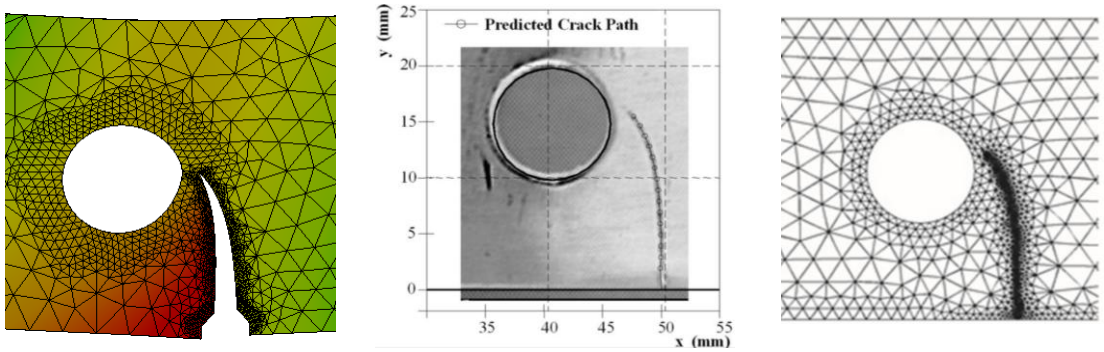

(a) (b) (c)

Figure 5. Crack growth path for 4SENB (a) Present study, (b) Experimental [25], and (c) Numerical using Quebra 2D [25].

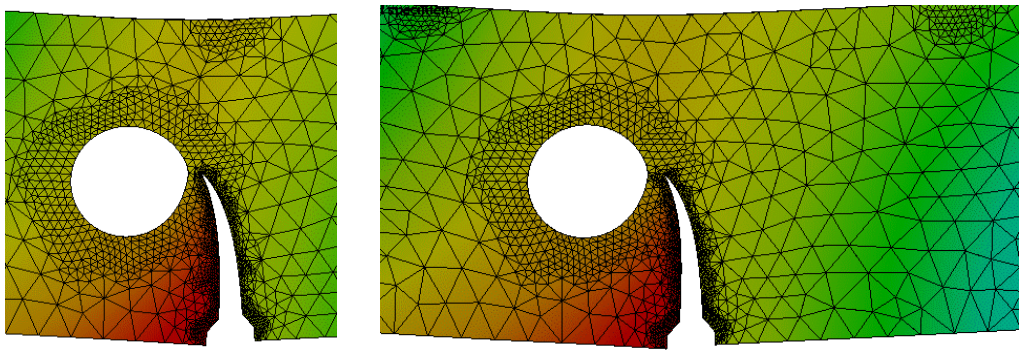

a b

Figure 6. Crack growth trajectory, (a) 3SENB and (b) 4SENB.

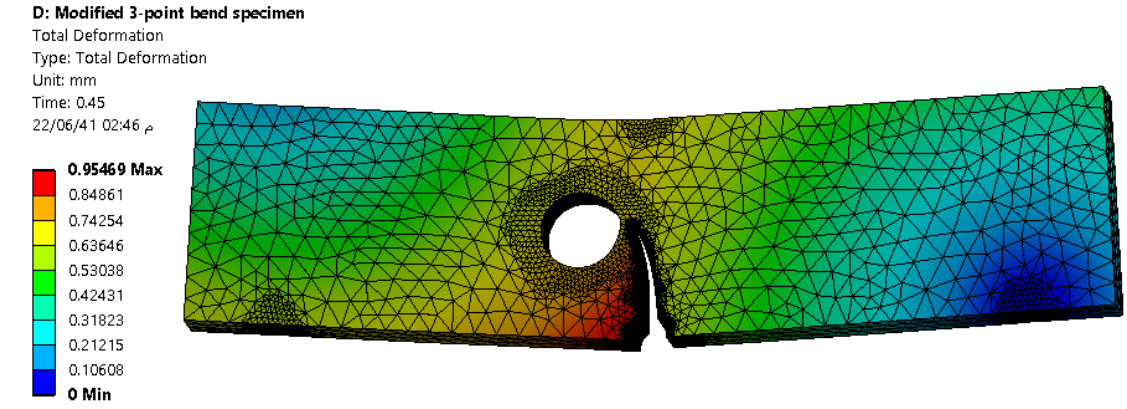

(a)

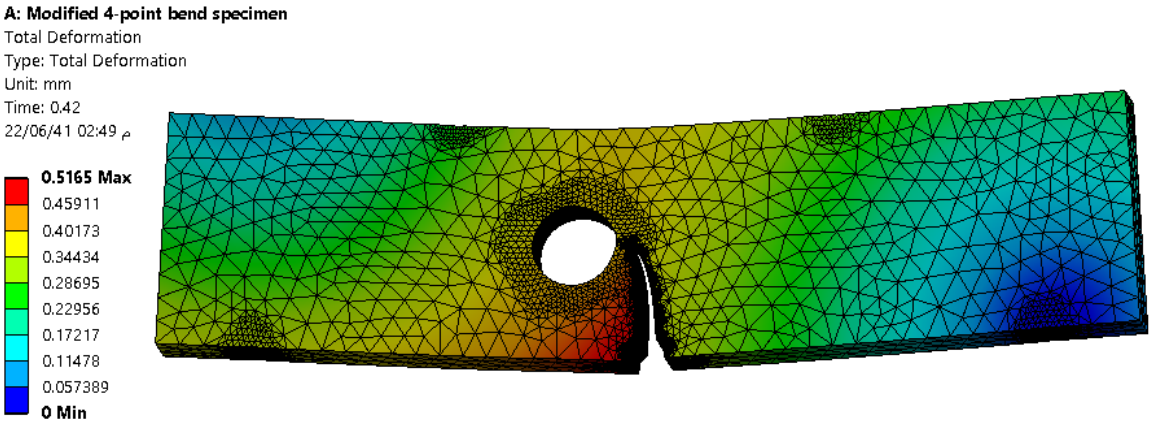

(b)

Figure 7. Total deformation (a) 3SENB and (b) 4SENB

The analysis of the SIFs provides the most critical quantitative validation of LEFM principles within the 3D computational framework. The threshold stress intensity factor for Mode I is the primary driver of crack propagation in these bending scenarios. According to the predicted values of the first mode of stress intensity factor as shown in Figure 8, for the 3SENB specimen, KI is calculated to be 693.15 MPa mm0.5, while the 4SENB specimen exhibits a value of 352.748 MPa mm0.5. Calculating the ratio reveals that the KI of the 3SENB has increased by a factor of 1.965. This scaling factor of 1.965 is remarkably close to the theoretical factor of 2.0 based on the doubling of the maximum bending moment.

The analysis of the Mode II SIF (K_{II}) highlights the mechanistic influence of the loading configuration. Generally, K_{II} values are similar for both specimens, indicating that Mode I dominance is preserved. However, a crucial localized difference exists: the K_{II} value in the 3SENB configuration is notably higher than that of the 4SENB configuration specifically at a crack length a=14.12 mm as displayed in Figure 9. This localized increase is directly attributed to the interaction between the structural geometry and the mechanical load distribution. At this precise crack length, the crack tip is beginning to be deflected by the stress field imposed by the eccentric hole (R = 5.2 mm, positioned 9.3 mm from the initial crack). Simultaneously, at this spatial location, the crack tip enters the region of the specimen that experiences the significantly higher shear force characteristic of the 3SENB configuration. This synergistic effect, the combination of geometric singularity (the hole) and high shear force, results in a transient, but influential, localized increase in the mixed-mode component (K_{II}). This finding is critical for understanding crack instability and potential path deviation in highly stressed zones.

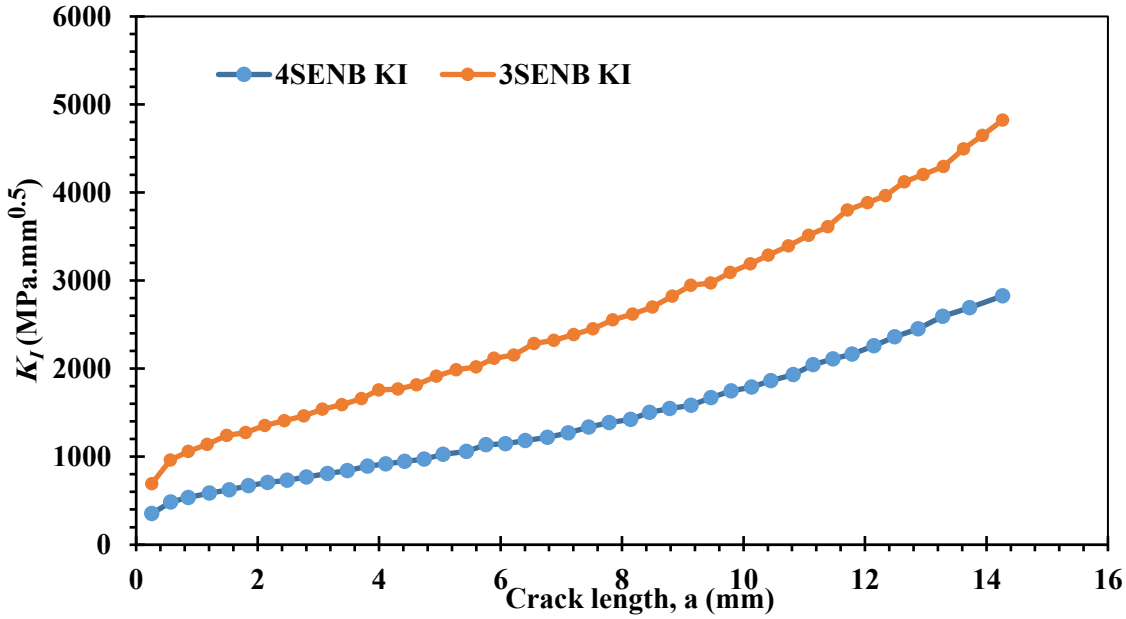

Figure 8. K_I versus crack length for the 3SENB and 4SENB.

The simulation results for the equivalent von-Mises stress and equivalent von-Mises strain demonstrate a strong, but not perfectly linear, correlation with the applied bending moment.

The maximum von-Mises stress recorded for the 3SENB specimen is 9313.6 MPa, which represents a factor of 1.931 increase over the maximum stress observed in the 4SENB specimen (4823.7 MPa) as shown in Figures 10 and 11 respectively. Similarly, the maximum von-Mises strain for the 3SENB configuration is 0.064119, which is an increase by a factor of 1.823 compared to the 4SENB value (0.035164) as shown in Figures 12 and 13 respectively. The fact that the scaling factors (1.931 for stress and 1.823 for strain) are very close to, but slightly less than, 2.0 is a significant finding. This deviation shows that simple linear scaling from far-field beam theory becomes slightly inaccurate over a complex 3D geometry comprising a sharp notch and a localized eccentric hole. Shifts in stress caused by the geometric discontinuities do not scale linearly. The result confirms the need for high-fidelity 3D finite element analysis (FEA) since these local effects would not be captured using simpler analytical models, which would not predict the correct non-linearity seen in the stress and strain fields. Analysing the specimens, 4SENB and 3SENB, it is possible to provide essential quantitative confirmation of the link between macroscopic loading (bending moment) and microscopic fracture parameters (SIFs), whilst also

bringing to light the different shear fields' mechanical consequences. The basic comparison confirms the objective of this study that has been carried out depicting a deliberate experimental design whereby the Mmax of the 3SENB specimen, Gets 500 KN.mm; and is exactly 2.0 times the M_{max} of the 4SENB specimen, which is 250 KN.mm as given in Figure 14. The shear force diagram depicted in Figure 15 indicates that for the 4SENB specimen, the shear force remains at zero value in the central region between the inner load points. In contrast, as you get closer to the load point, shear force of 3SENB is continuously increasing. The shear force of 3SENB from the distance of 37.5 mm to 87.5 mm along the length of the beam is significantly higher compared to that of 4SENB. The interpretation of the Mode II SIF results hinges on this observation. Table 3 reveals a direct correlation between the bending moment and main fracture parameters in the form of proportional scaling.

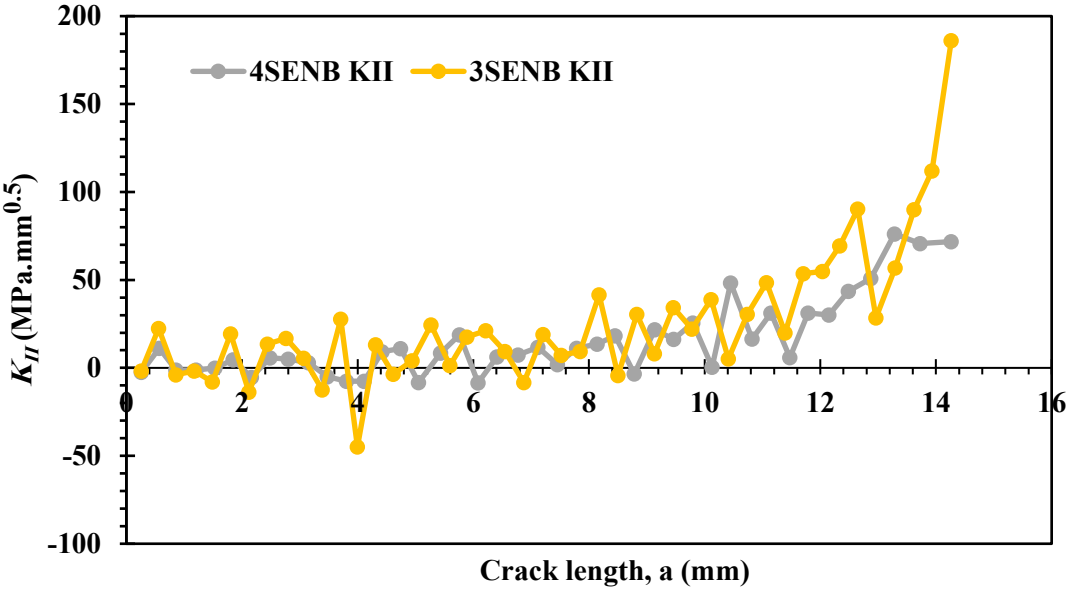

Figure 9. Predicted values of the second mode of SIF 3SENB and 4SENB.

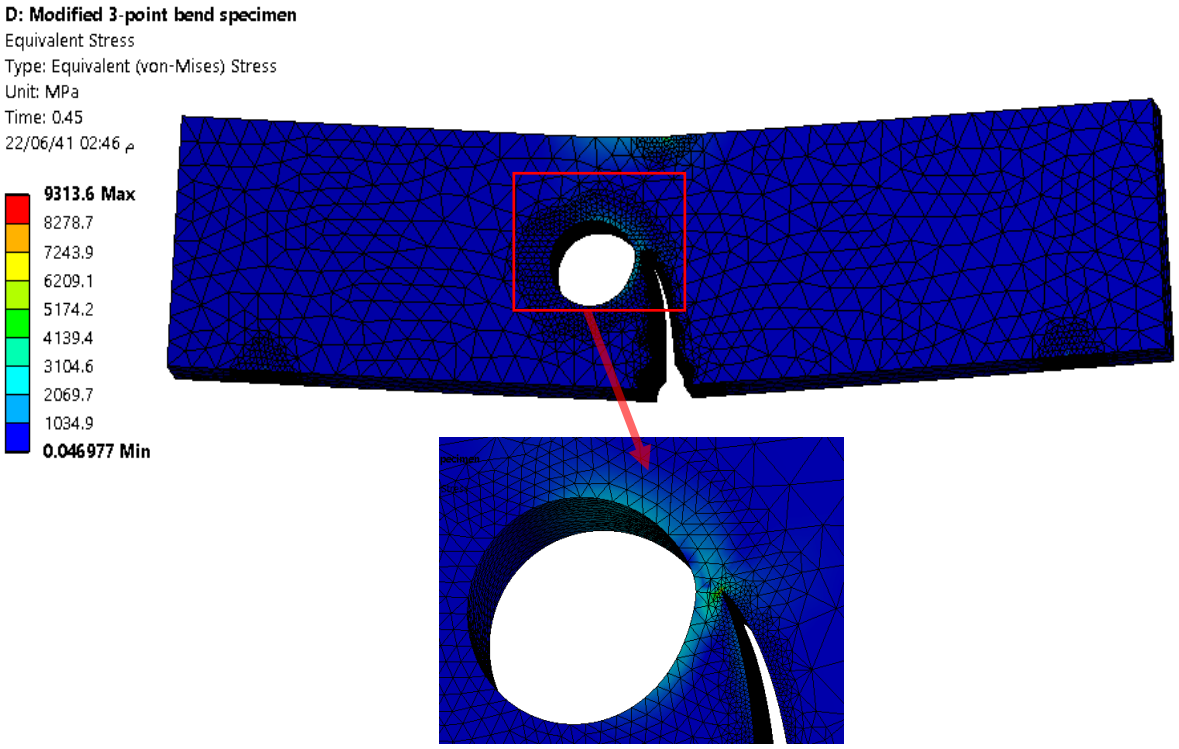

Figure 10. Predicted values for the equivalent (von-Mises) stress of the 3SENB specimen.

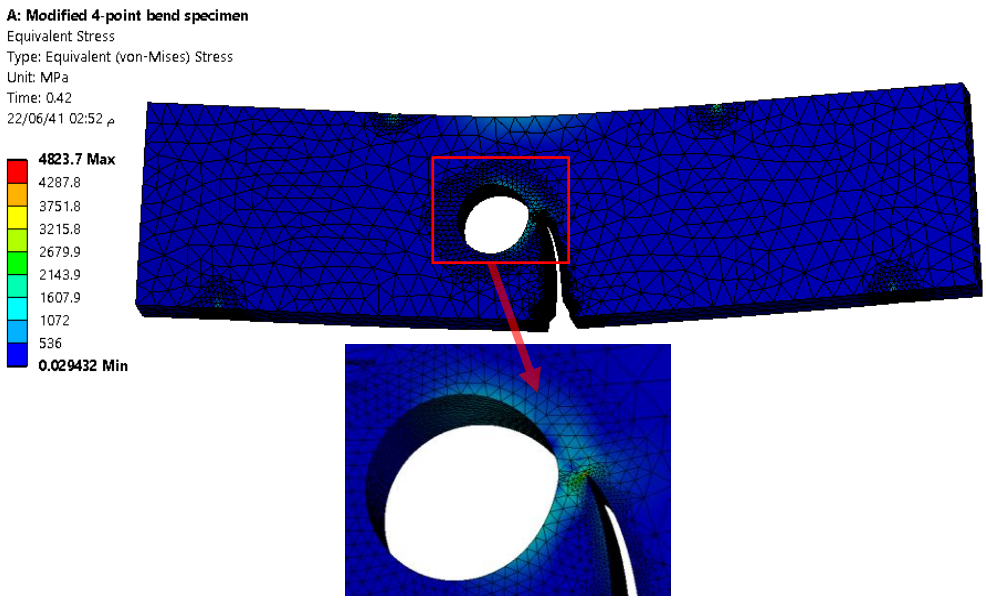

Figure 11. Predicted values for the equivalent (von-Mises) stress of the 4SENB specimen.

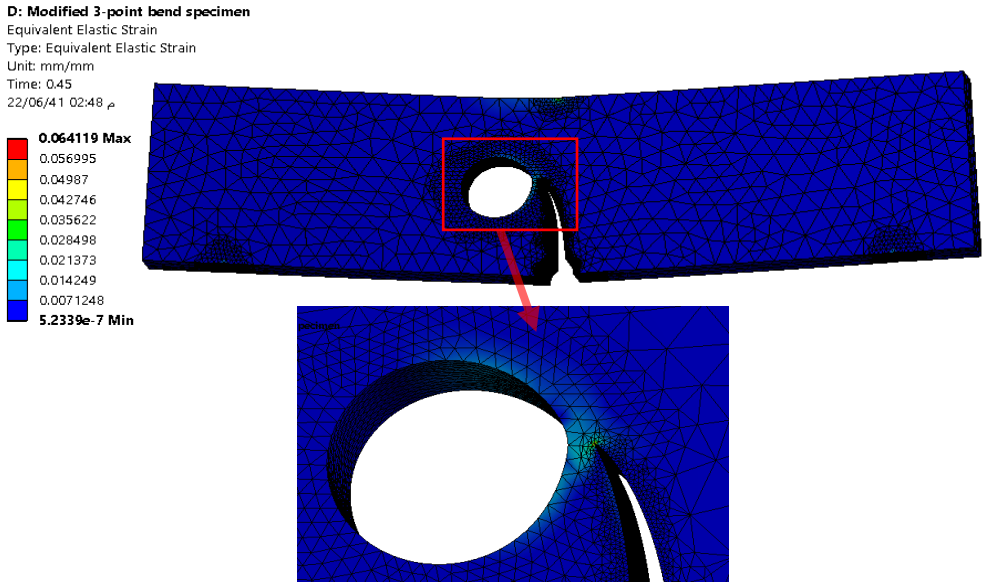

Figure 12. Equivalent (von-Mises) strain for the 3SENB specimen.

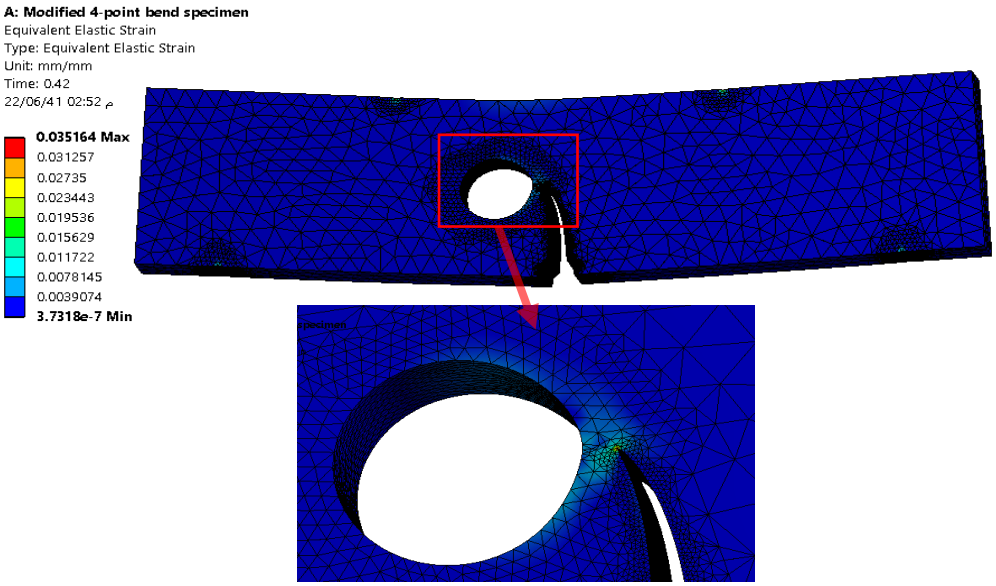

Figure 13. Equivalent (von-Mises) strain for the 4SENB specimen.

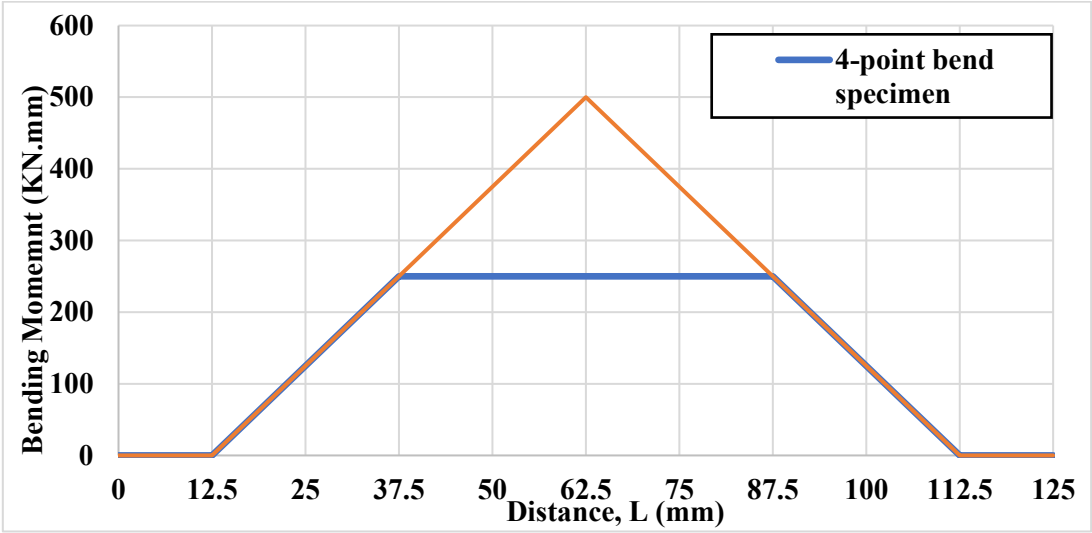

Figure 14. Bending moment diagram for the 4SENB and 3SENB.

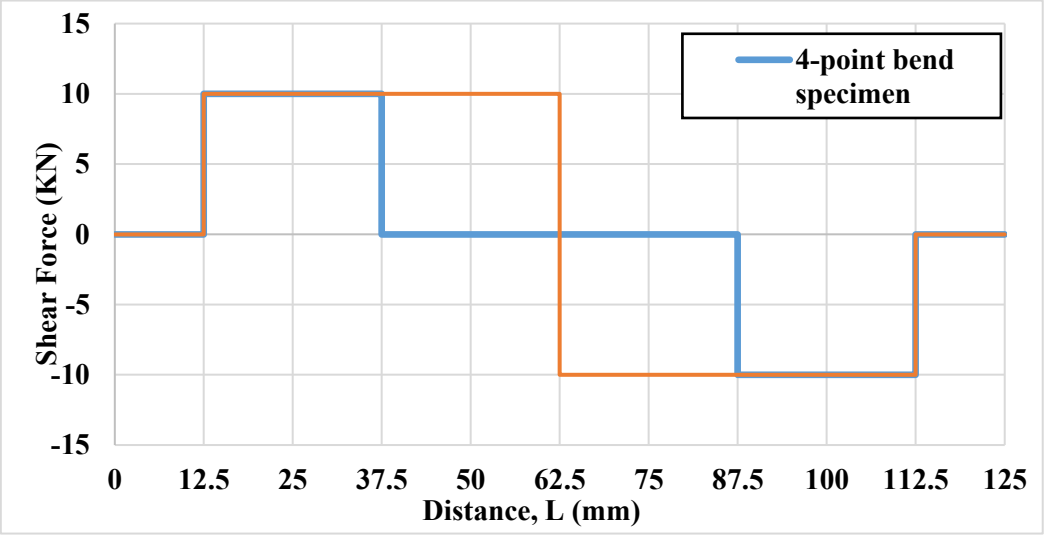

Figure 15. Shear force diagram for the 4SENB and 3SENB.

Table 3 summarizes the influence of the bending moment on the primary fracture parameters, highlighting the proportional scaling factors. The obtained numerical data plotted in Figure 16 as crack length versus number of loading cycles shows a clear difference in the crack propagation kinetics of 3SENB and 4SENB specimens under the same cyclic loading conditions. The first important finding suggests that the mechanical environment created by the three-point bending arrangement consistently increases the rate of crack propagation, denoted as (da/dN). The 3SENB specimen did not pass the test after 3.24 × 105 cycles. Different from previous behavior, the specimen 4SENB reached the equivalent failure criterion after sustaining a load of 4.36 × 105 cycles. Under the ANSYS simulation carried out, there is a decrease of no less than 34% in total fatigue life for 3SENB.

Table 3. Comparative Analysis of Maximum Fracture Parameters of 3SENB and 4SENB.

Modified SENB specimen	Max. Bending Moment	Max. von-Mises Stress	Max. von-Mises Strain	K_{Ith}
4SENB	250 KN.mm	4823.7 MPa	0.035164	352.748 MPa.mm$^{0.5}$
3SENB	500 KN.mm	9313.6 MPa	0.064119	693.15 MPa.mm$^{0.5}$
$\frac{\textbf{3SENB}}{\textbf{4SENB}}$	2	1.931	1.823	1.965

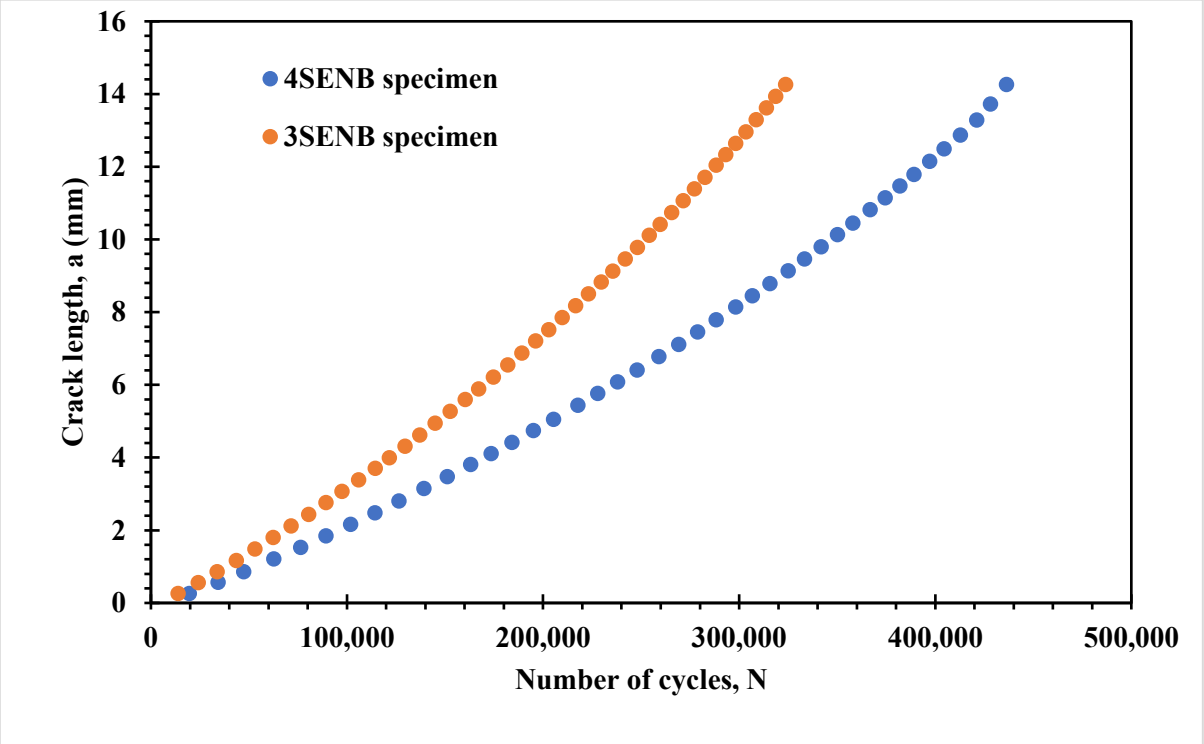

Figure 16. Fatigue life cycles for 4SENB and 3SENB.

4. CONCLUSION

A detailed numerical study of a modified Single Edge Notched Bend (SENB) specimen with a geometric discontinuity situated near the crack tip is presented. This study performed a comparative numerical analysis for modified SENB using finite element method in ANSYS Workbench. This specimen which possessed a geometrical discontinuity at the crack tip was assessed under 3SENB and 4SENB loading cases. The novelty of this work lies in the direct, quantitative comparison of how the different types of loading affect the fracture mechanics parameters of this non-standard geometry, which is often not covered in the standard tests.

The analysis yielded several significant findings regarding the specimen's structural response and fatigue behaviour:

1- A strong and nearly linear relationship has been established between the maximum bending moment and the parameters of fracture. In the 3SENB model, the maximum bending moment was two-fold greater than that in the 4SENB one. In precise terms, the maximum von Mises stress (a factor of 1.931), maximum von Mises strain (a factor of 1.823), and the KIth (a factor of 1.965). This gives an important engineering guidance on deriving the severity of a loading condition based on the maximum bending moment for this class of modified geometries.

2- The stress intensity factors and localised stress concentrations that occur in a 3SENB specimen are greater than that of the 4SENB specimen. Thus, the fatigue life in the numerical analysis would be substantially lower in a 3SENB specimen.

3- The loading configuration plays a crucial role in assessing the integrity of the structure.

The numerical model showed high fidelity and the predicted crack path compared well to the external numerical and experimental data of other researchers. The path of the crack did not appear to be affected by the different loading configuration.

REFERENCES

[1] Demiral, Murat. "Strength in Adhesion: A Multi-Mechanics Review Covering Tensile, Shear, Fracture, Fatigue, Creep, and Impact Behavior of Polymer Bonding in Composites." *Polymers* 17, no. 19 (2025): 2600. https://doi.org/10.3390/polym17192600

[2] Zeng, Yong, Hongwei He, Yu Qu, Xudong Sun, Hongmei Tan, and Jianting Zhou. "Numerical Simulation of Fatigue Cracking of Diaphragm Notch in Orthotropic Steel Deck Model." *Materials* 16, no. 2 (2023): 467. https://doi.org/10.3390/ma16020467

[3] Anderson, Ted L. *Fracture Mechanics: Fundamentals and Applications*: CRC press, 2017.

[4] Li, Linfeng, Haytham F Isleem, Mohammad Khishe, and Ghanshyam G Tejani. "A Comparative Study of Machine Learning Methods for Predicting Mode I and Ii Brittle Fracture in Notched Bend Specimens." *Scientific Reports* 15, no. 1 (2025): 36406. https://doi.org/10.1038/s41598-025-20349-3

[5] Wang, Shuaiqiang, and WU Zhirong. "Numerical Simulation of Fatigue Crack Growth Life of Single Side Notched Specimen." Paper presented at the Journal of Physics: Conference Series 2021. https://doi.org/10.1088/1742-6596/1965/1/012122

[6] Fett, Theo. *An Analysis of Stresses and Stress Intensity Factors in 3-and 4-Point Bending Bars*: FZKA, 1998.
[7] Unuk, Žiga, and Milan Kuhta. "Nonlinear Semi-Numeric and Finite Element Analysis of Three-Point Bending Tests of Notched Polymer Fiber-Reinforced Concrete Prisms." *Applied Sciences* 14, no. 4 (2024): 1604. https://doi.org/10.3390/app14041604
[8] Tseng, Ampere A. "A Three-Dimensional Finite Element Analysis of the Three-Point Bend Specimen." *Engineering Fracture Mechanics* 13, no. 4 (1980): 939-43. https://doi.org/10.1016/0013-7944(80)90023-5
[9] Husnain, MNM, JQ Lee, MRM Akramin, MS Shamil, and Akiyuki Takahashi. "Finite Element Analysis of Bending Tests for Fatigue Cracking Assessment." *Journal of the Brazilian Society of Mechanical Sciences and Engineering* 47, no. 8 (2025): 363. https://doi.org/10.1007/s40430-025-05574-1
[10] Ganguwar, S, and VM Nistane. "Study on Comparison between Three Point Bending and Four Point Bending Test Condition for Functionally Graded Material Beam with Crack." *Strength, Fracture and Complexity* 18, no. 1 (2025): 18-31. https://doi.org/10.1177/15672069241304945
[11] Rahim, Mohammad Ridzwan Bin Abd, Siegfried Schmauder, Yupiter HP Manurung, Peter Binkele, Ján Dusza, Tamás Csanádi, Meor Iqram Meor Ahmad, Muhd Faiz Mat, and Kiarash Jamali Dogahe. "Assessing Fatigue Life Cycles of Material X10crmovnb9-1 through a Combination of Experimental and Finite Element Analysis." *Metals* 13, no. 12 (2023): 1947. https://doi.org/10.3390/met13121947
[12] Yahia, Abul Kashem Mohammad, and Mohammad Shahjalal. "Recent Developments and Challenges in Fracture Mechanics–Based Fatigue Life Prediction." *ASRC Procedia: Global Perspectives in Science and Scholarship* 1, no. 01 (2025): 1202-37. https://doi.org/10.63125/qgtnp591
[13] Fageehi, Y. A., and Abdulnaser M Alshoaibi. "Comparative Finite Element Analysis of Fatigue Crack Growth in High-Performance Metallic Alloys: Influence of Material Parameters and Paris' law Constants." *Crystals* 15, no. 9 (2025): 801. https://doi.org/10.3390/cryst15090801
[14] Fageehi, Y.A., and Abdulnaser M Alshoaibi. "Modeling Fatigue Crack Growth under Compressive Loads: The Role of Non-Monotonic Stress and Crack Closure." *Crystals* 15, no. 11 (2025): 979. https://doi.org/10.3390/cryst15110979
[15] Gupta, A, W Sun, and CJ Bennett. "Simulation of Fatigue Small Crack Growth in Additive Manufactured Ti–6al–4v Material." *Continuum Mechanics and Thermodynamics* 32, no. 6 (2020): 1745-61. https://doi.org/10.1007/s00161-020-00878-0
[16] Chen, Bao, Sun Yongduo, Wu Yuanjun, Wang Kaiqing, Wang Li, and He Guangwei. "Fracture Properties and Crack Tip Constraint Quantification of 321/690 Dissimilar Metal Girth Welded Joints by Using Miniature Senb Specimens." *Nuclear Engineering and Technology* 53, no. 6 (2021): 1924-30. https://doi.org/10.1016/j.net.2020.12.020
[17] Damjanović, D., Kozak, D., Matvienko, Y., & Gubeljak, N. (2017). Correlation of Pipe Ring Notched Bend (PRNB) specimen and Single Edge Notch Bend (SENB) specimen in determination of fracture toughness of pipe material. Fatigue & fracture of engineering materials & structures, 40(8), 1251-1259. https://doi.org/10.1111/ffe.12581
[18] Gonzalez, Marco, Paulo Teixeira, Jeanette Gonzalez, and Raul Machado. "Numerical Analysis of Fracture Mechanics of Senb Specimens Prepared from HDPE Pipes." Paper presented at the Pressure Vessels and Piping Conference 2014. https://doi.org/10.1115/PVP2014-28718
[19] Neto, DM, N Cavaleiro, Edmundo R Sérgio, J Jesus, A Camacho-Reyes, and FV Antunes. "Effect of Crack Flank Holes on Fatigue Crack Growth." *International Journal of Fatigue* 170 (2023): 107505. https://doi.org/10.1016/j.ijfatigue.2023.107505
[20] Kim, Sang Jin, Jung Min Sohn, and Do Kyun Kim. "Effect of Cracks on the Compressive Ultimate Strength of Plate and Stiffened Panel under Biaxial Loads: A Finite Element Analysis." *Applied Sciences* 15, no. 15 (2025): 8287. https://doi.org/10.3390/app15158287
[21] Ferreira, Denis Alves, Vagner Pascualinotto Junior, and Diego FB Sarzosa. "Test Protocol Definition to Measure Fracture Toughness J-Parameter Using Non-Standard Four-Point Bending Specimens." Paper presented at the Pressure Vessels and Piping Conference 2020. https://doi.org/10.1115/PVP2020-21592
[22] Ferreira, Denis A, Rafael Savioli, and Diego FB Sarzosa. "New Formulation for Fracture Toughness Characterization Using Four-Point Bend Specimens." *Engineering Fracture Mechanics* 241 (2021): 107409. https://doi.org/10.1016/j.engfracmech.2020.107409
[23] Pereira, Sérgio Alexandre Gonçalves, Sérgio MO Tavares, and Paulo MST de Castro. "Mixed Mode Fracture: Numerical Evaluation and Experimental Validation Using Pmma Specimens." *Fracture and Structural Integrity* 13, no. 49 (2019): 412-28. https://doi.org/10.3221/IGF-ESIS.49.40
[24] Miranda, ACO, MA Meggiolaro, JTP Castro, LF Martha, and TN Bittencourt. "Fatigue Life and Crack Path Predictions in Generic 2d Structural Components." *Engineering Fracture Mechanics* 70, no. 10 (2003): 1259-79. https://doi.org/10.1016/S0013-7944(02)00099-1
[25] Gomes, Gilberto, and Antonio CO Miranda. "Analysis of Crack Growth Problems Using the Object-Oriented Program Bemcracker2d." *Frattura ed Integrità Strutturale* 12, no. 45 (2018): 67-85. https://doi.org/10.3221/IGF-ESIS.45.06